Journal of Materials Chemistry C

Accepted Manuscript

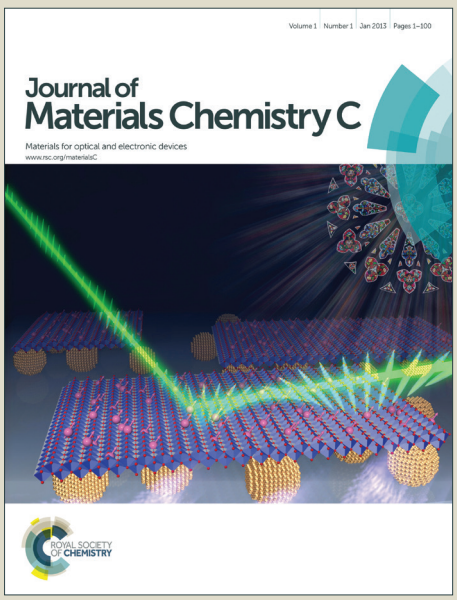

ROYAL SOCIETY OF CHEMISTRY

www.rsc.org/materialsC

Journal Name

ARTICLE

Luminescence and energy transfer of $Eu^{2+}/Tb^{3+}/Eu^{3+}$ in $LiBaBO_3$ phosphors with tunable-color emission

Received 00th January 20xx,
Accepted 00th January 20xx

DOI: 10.1039/x0xx00000x
www.rsc.org/

Shuchao Xu, Panlai Li*, Zhijun Wang*, Ting Li, Qiongyu Bai, Jiang Sun, Zhiping Yang

Abstract: A series of $LiBaBO_3$:RE (RE=$Eu^{2+}/Tb^{3+}/Eu^{3+}$) phosphors had been synthesized by the high-temperature solid-state reaction method. The X-ray diffraction (XRD), emission spectra, excitation spectra, decay lifetimes, and diffuse reflection spectra were utilized to characterize the phosphors. The as-prepared samples had been demonstrated via XRD measurement and showed that the $Eu^{2+}/Tb^{3+}/Eu^{3+}$ can be efficiently doped into the host. The obtained phosphors can emit different colors light when doping with different activators. The energy transfer from Tb^{3+} to Eu^{3+} occurs in $LiBaBO_3$:$0.03Eu^{3+}$, yTb^{3+} prepared in the air. While an abnormal reduction phenomenon was reported when Eu and Tb ions were co-doped in $LiBaBO_3$ and prepared in an inferior reductive atmosphere, which showed tunable-color from blue to red based on energy transfer of $Eu^{2+}\rightarrow Tb^{3+}\rightarrow Eu^{3+}$ ions. And the energy transfer not only can occur between Eu^{2+} and Tb^{3+} ions, but also Tb^{3+} and Eu^{3+} ions. All these results reveal that Tb^{3+} can play the role of storing the energy for Eu^{3+}, and $LiBaBO_3$ may be potential candidate phosphors for LEDs.

1. Introduction

Rare earth elements and transition metal ions act as important activators doped in phosphors for application in modern lighting and display fields due to their abundant emission colors to achieve spectra conversion [1]. Especially, Eu is the most commonly used activator because both Eu^{3+} and Eu^{2+} can function as an emission center in the host lattices [2-5]. The sensitivity of the energy transformation between 4f and 5d energy levels of Eu^{2+} permits possibility to achieve tunable luminescence, in addition, for Eu^{2+} ions, the decay time is short, making the Eu^{2+} a popular activator [6-9]. The Tb^{3+} ion is regarded as a promising green-emitting activator for showing sharp lines at about 497, 550, and 597nm due to the 4f−4f transition. As is well-known in the lighting community, Eu^{3+} can produce efficient red emission around 615 nm due to the $^5D_0 \rightarrow {}^7F_2$ transition and this has been applied in commercial red phosphors for decades like Y_2O_3:Eu^{3+} and Y_2O_2S:Eu^{3+}. It is very significant to develop Eu^{3+} doped phosphors for light emitting diode (LED) applications, but the weak absorption of Eu^{3+} in the blue and near-ultraviolet (UV) has limited use in practical LED systems. An effective way to solve the above problem is by utilizing energy transfer from sensitizers to activators in a proper host [10-12]. Since the Eu^{2+} and Tb^{3+} ion may be good sensitizers for the Eu^{3+} ion, it is important to study luminescence and energy transfer of the Eu^{2+}, Tb^{3+}, Eu^{3+} co-doped phosphors [13].

In this study, we investigated the luminescence properties of $Eu^{2+}/Tb^{3+}/Eu^{3+}$ activated $LiBaBO_3$. The solid-state reaction to synthesis the host was employed here and we obtained different co-doped phosphors under different conditions. The obtained phosphors exhibited good emission properties when individually activated with Eu^{3+}, Tb^{3+} or Eu^{2+} ions. Besides, under inferior reductive atmosphere, we find Eu^{2+}, Tb^{3+} and Eu^{3+} can coexist in the host, and the co-activated phosphors showed tunable emission based on the concentration of activator ions and the selection of excitation energy. Our studies indicate that the coexistence of Eu^{3+}, Tb^{3+} and Eu^{2+} in $LiBaBO_3$ phosphors show rich optical properties, which might be a promising material for LEDs with vivid color emissions.

2. Experimental

2.1. Materials and synthesis

All the phosphors with compositions of $LiBaBO_3$:xEu, yTb described in this work were obtained by a solid-state reaction. In other words, the constituent raw materials Li_2CO_3 (A.R.), $BaCO_3$ (A.R.), H_3BO_3 (A.R.), Eu_2O_3 (99.99%) and Tb_4O_7 (99.99%) were weighed in stoichiometric proportions (using the ratio of synthetic quantity) and completely mixed and ground into powder in an agate mortar. Then, the mixture was transferred into an alumina crucible and heated at 700℃ for 3h. Finally, all the mixture grounded again into powder for measurement. The specific chemical equations and the synthetic conditions can be expressed as follows:

Hebei Key Lab of Optic-electronic Information and Materials, College of Physics Science & Technology, Hebei University, Baoding 071002, China
† li_panlai@126.com; wangzj1998@126.com
Electronic Supplementary Information (ESI) available: [details of any supplementary information available should be included here]. See DOI: 10.1039/x0xx00000x

We obtained $LiBaBO_3$:xEu^{2+} and $LiBaBO_3$:yTb^{3+} phosphors (in reductive atmosphere, 95%H_2+5%N_2), $LiBaBO_3$:xEu^{3+} and $LiBaBO_3$:yTb^{3+} (in air), respectively, the reaction as follows:

$Ba_{1-x}CO_3+\frac{1}{2}Li_2CO_3+H_3BO_3+\frac{x}{2}Eu_2O_3 \rightarrow LiBaBO_3:xEu$

$Ba_{1-y}CO_3+\frac{1}{2}Li_2CO_3+H_3BO_3+\frac{y}{4}Tb_4O_7 \rightarrow LiBaBO_3:yTb$

We prepared $LiBaBO_3$:$0.03Eu^{3+}$, yTb^{3+} (in air), the reaction as follows:

$Ba_{1-0.03-y}CO_3+\frac{1}{2}Li_2CO_3+H_3BO_3+\frac{0.03}{2}Eu_2O_3+\frac{y}{4}Tb_4O_7 \rightarrow LiBaBO_3:0.03Eu^{3+}$, yTb^{3+}

We achieved Eu^{2+} and Eu^{3+} coexisted in $LiBaBO_3$ phosphors (in an inferior reductive atmosphere, i.e., in the carbon dust), the reaction as follows:

$Ba_{1-x}CO_3+\frac{1}{2}Li_2CO_3+H_3BO_3+\frac{x}{2}Eu_2O_3 \rightarrow LiBaBO_3:x(Eu^{2+}, Eu^{3+})$

We synthesized Eu^{2+}, Eu^{3+} and Tb^{3+} coexisted in $LiBaBO_3$ phosphors (in an inferior reductive atmosphere, i.e., in the carbon dust), the reaction as follows:

$Ba_{1-0.03-y}O_3+\frac{1}{2}Li_2CO_3+H_3BO_3+\frac{0.03}{2}Eu_2O_3+\frac{y}{4}Tb_4O_7 \rightarrow LiBaBO_3:0.03(Eu^{2+}, Eu^{3+}), yTb^{3+}$

2.2. Materials characterization

The phase structures of the as-prepared samples, i.e., X-ray diffraction (XRD) were carefully performed on D8-A25 Focus diffractometer (Bruker) measuring at 40KV and 40mA and recording the patterns in the range, 2θ = 20 ° to 80 °with scan rate of 0.05 °/s. Measurements of excitation and emission spectra were recorded with a HITACHI F-4600 fluorescence spectrophotometer using a Xe lamp as the excitation source, scanning at 240 nm/min. The decay curves of Eu^{3+} and Tb^{3+} with HORIBA FL-1057 equipped with a Xe lamp as the excitation source while Eu^{2+} with FLS920 produced in Edinburgh Instruments with a microsecond lamp as the excitation source. Diffuse reflection spectra on the phosphors were surveyed on a HITACHI U4100 machine, at a scanning wavelength range of 200–800 nm. All these above measurements were performed at room temperature.

3. Results and discussions

3.1. Crystallization behaviour and structure

The XRD patterns of samples are measured and a similar diffraction patterns are observed for each sample. As a representative, Figure1 shows the XRD patterns of $LiBaBO_3$:$0.03Eu^{3+}$, $LiBaBO_3$:$0.03Tb^{3+}$, $LiBaBO_3$:$0.03Eu^{3+}$, $0.03Tb^{3+}$, $LiBaBO_3$:$0.03Eu^{3+}$, $0.10Tb^{3+}$, $LiBaBO_3$:$0.10Eu^{3+}$, $0.03Tb^{3+}$. All the diffraction peaks of these prepared samples can be assigned to pure monoclinic cell of $LiBaBO_3$, in other words, they match well with the standard values of PDF card (JCPDS no.81-1808), indicating that the doped Eu, Tb ions have no impact on the host structure. Considering the ionic radii of Li^+ (0.59 Å) and Ba^{2+} (1.35 Å), we suppose that the rare earth ions (1.25 Å for Eu^{2+}, 1.01 Å for Eu^{3+} and 1.095 Å for Tb^{3+}) are expected to occupy the site of Ba ion[14-16]. From Figure 1 we can also see that the diffraction peaks of the phosphors have a little difference with the doping of rare earth ions. This phenomenon is associated with the substituting of larger Ba ions by smaller Eu and Tb ions and can reflect that the doped ions are completely incorporated into the host. All peaks can be successfully indexed by a monoclinic cell (P21/c) with parameters close to reported value of $LiBaBO_3$ and the fitting obtained cell parameters of a = 6.372 Å, b = 7.022 Å, c = 7.058 Å, β = 113.89 °, and Z= 4. Figure 2 (a) shows the unit cell structure of $LiBaBO_3$; (b) shows the ion bond between B, O, Ba and Li, and we see that Li, Ba, and B connected via O ion; (c) shows the ion bond between B and O, and the distance is 1.373 Å, 1.378 Å, 1.390 Å with the angle is 122.50 °, 118.49 °, 119.00 °, respectively.

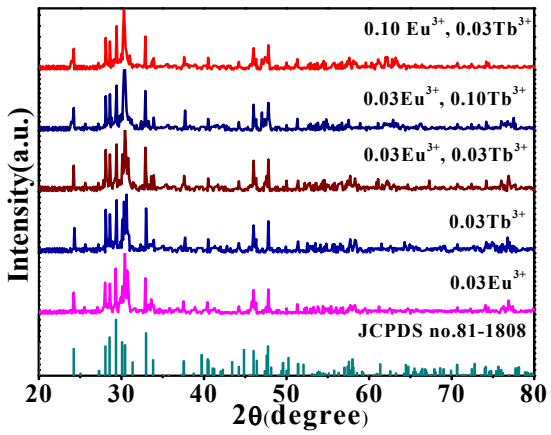

Figure 1 XRD patterns of $LiBaBO_3$:RE (RE = Eu/Tb) samples. The standard pattern of $LiBaBO_3$ (JCPDS no. 81-1808) is provided as reference.

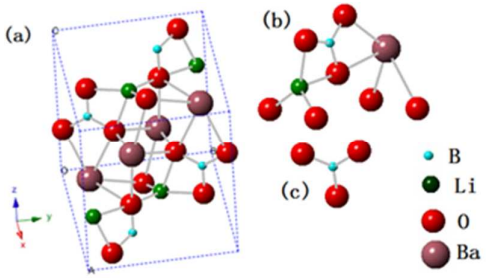

Figure 2 Unit cell representation of the crystal structure of $LiBaBO_3$ .Blue, green, red, purple represent B, Li, O, and Ba atoms, respectively.

3.2. Reflectance spectra of host

The reflectance spectra of inferior reductive $LiBaBO_3$:*x*Eu (*x* =0, 0.03, 0.05, 0.10), reduced and non-reduced $LiBaBO_3$:0.03Tb and inferior reductive $LiBaBO_3$:0.03Eu, *y*Tb (*y*=0.03, 0.05, 0.07) phosphors were shown in Figure 3 (a) (b) and (c). From Figure 3 (a) (b) and (c), we observed the reflectance spectra curve trend is substantially the same, that is, the diffuse reflection spectrum of the $LiBaBO_3$ host shows a status of high reflection in the wavelength ranging from 400 to 800 nm, and decreasing intensity from 300 to 400 nm that can be attributed to the host absorption band. For the reason that their tendencies are substantially the same, I chose inferior reductive $LiBaBO_3$:xEu to calculate the host absorption

band. The Kubelka-Munk absorption coefficient (K/S) relation is used to calculate the measured reflectance (R) for the host lattice.

$$\frac{K}{S}=\frac{(1-R)^2}{2R} \quad (1)$$

where K represents the absorption coefficient, S the scattering coefficient, and R the reflectivity. The fundamental band gap energy (absorption edge) of the $LiBaBO_3$ host was calculated to be approximately 2.90eV (427nm) from the K/S relation spectrum by extrapolation, as given in Figure 3 (d). Obvious differences appear in the spectral profiles of ions-doped samples compared to that of the host. The strong broad absorption appeared in the 300-420 nm near-UV range, which was attributed to the electronic transition absorption of the ions. The absorption intensities increase gradually with the increasing ion concentrations and the absorption intensity of non-reduced host significantly greater than reduced host.

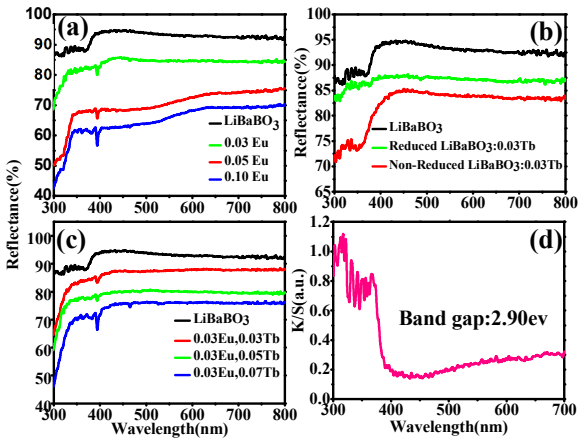

Figure 3 (a), (b) and (c) represent the diffuse reflectance spectra of inferior reductive $LiBaBO_3$:*x*Eu (*x* =0, 0.03, 0.05, 0.10), reduced and non-reduced $LiBaBO_3$:0.03Tb and inferior reductive $LiBaBO_3$:0.03Eu, *y*Tb (*y*=0.03, 0.05, 0.07) phosphors respectively, and (d) shows Kubelka–Munk absorption spectrum for $LiBaBO_3$ host.

3.3. Luminescence properties of Eu doped materials

Figure 4(a) and (b) depicts the emission and excitation spectra of the sintered non-reductive (in the air) and reductive (in the atmosphere of 95%H_2+5%N_2) $LiBaBO_3$:*x*Eu phosphor together with their corresponding photograph under 365 nm UV lamp. And the spectrums changing with the concentration of Eu^{3+} is shown in Figure S1. By the spectra, the Eu^{3+} luminescence can be distinctly separated from Eu^{2+} as displayed in Figure 4(a) and (b). From (a), it can be seen Eu^{3+} ions show typical emission lines and the spectral region of 580–730 nm corresponding $^5D_0$–^7F_J (J = 0, 1, 2, 3, and 4) transitions with its typical red light. Figure (b) shows an intense blue emission band attributed to the $^4f_6{}^5d_1 \rightarrow {}^4f_7$ transition from 400 to 600 nm comes from the emissions of Eu^{2+} ions and when monitored at 500 nm which is the excitation energy of Eu^{2+}, the sample shows a broad intense band from 280 to 430 nm with a maximum at 350 nm which is due to the $^4f_7 \rightarrow {}^4f_6{}^5d_1$ transition of Eu^{2+} ions, for the reason that although Eu^{2+} have complicated set of energy levels it and can emit a very broad spectrum, due to the involvement of seven 4f-electrons [17], the energies of the 4f-5d transitions are the lowest in Eu^{2+} [18], and it will behave differently and emit different colors of light in different hosts, moreover, the band gap of $LiBaBO_3$ is 2.90 ev which is very close to the crystal field splitting for Eu^{2+} on the octahedral Ba-site(2.70 ev) and Eu^{2+} occupies octahedral sites in $LiBaBO_3$ [18]. However, when prepared $LiBaBO_3$:*x*Eu in an inferior reductive atmosphere (in the carbon dust), the typical emission peak of $Eu^{2+}$and Eu^{3+} can be found at the same condition in the host. Figure(c) shows the PL spectra of the inferior reductive $LiBaBO_3$:*x*Eu with different concentrations and their corresponding photographs under 365 nm UV lamp. It has been established that $^4f_7 \rightarrow {}^4f_6{}^5d_1$ emission transitions of Eu^{2+} and in a compound are allowed, resulting in broad luminescence spectra and a very short lifetime in microsecond regions which will be introduced as following, and the sharp emission peaks in the range from 580 to 730 nm belong to the f–f transitions of $^5D_0$–^7F_J (J = 0, 1, 2, 3, and 4) of Eu^{3+}, with a lifetime longer than several millisecond which also will be introduced as following. We can infer the coexistence of $Eu^{2+}$and Eu^{3+} in the host. Since the non-doped sample of $LiBaBO_3$ does not show any light, the gradual change of the color also prove that the coexistence of $Eu^{2+}$and Eu^{3+}.

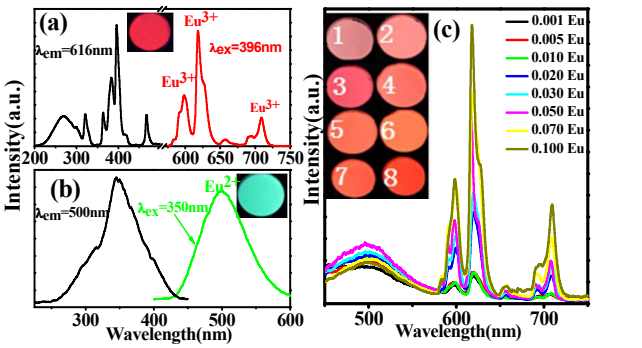

Figure 4 Emission and excitation spectra of $LiBaBO_3$:0.10Eu prepared in the air (a) and reductive atmosphere (H_2+N_2) (b) and emission spectra of $LiBaBO_3$:xEu phosphors prepared in an inferior reductive atmosphere (in the carbon dust) together with their corresponding photographs under 365 nm UV lamp.

To further illustrate the Eu^{2+} ions and Eu^{3+} ions can coexist in the host of $LiBaBO_3$, the decay time of the inferior reductive $LiBaBO_3$:*x*Eu were measured. The decay curves of $Eu^{3+}$and Eu^{2+} in $LiBaBO_3$:*x*Eu (*x* =0.03, 0.05, 0.07, 0.10) excited at 396 nm and 350 nm are measured and depicted in Figure 5 and Figure 6. The Eu^{3+} decay curves were fitted to a single exponential function and the Eu^{2+} decay curves were fitted to quadratic exponential function. The average lifetimes of the single exponential curves (Eu^{3+}) was calculated by the formula given in the following:

$$y=A\exp(-x/t)+y_0 \quad (2)$$

where A and y_0 are constants, t is the lifetimes. The calculated lifetimes are presented in Figure 5. And the average lifetimes of the quadratic exponential curves (Eu^{2+}) was calculated by the formula given in the following [19]:

$$t = (A_1t_1^2 + A_2t_2^2)/(A_1t_1 + A_2t_2) \quad (3)$$

where A_1 and A_2 are constants, t_1 and t_2 are the short and long lifetimes. The calculated lifetimes are presented in Figure 6. From the decay time, the Eu^{3+} luminescence can be distinctly separated from Eu^{2+} as displayed in Figure 5 and Figure 6. The longer lifetime than several millisecond belongs to the emission transitions from Eu^{3+} ions. And the shorter lifetime of Eu^{2+} also can be observed after laser excitation. This indicates that actually two valence states, +2 and +3, are available for Eu ions. Therefore, we can conclude that Eu^{2+} and Eu^{3+} can coexist in the host under the preparation in inferior-reduction at high temperature.

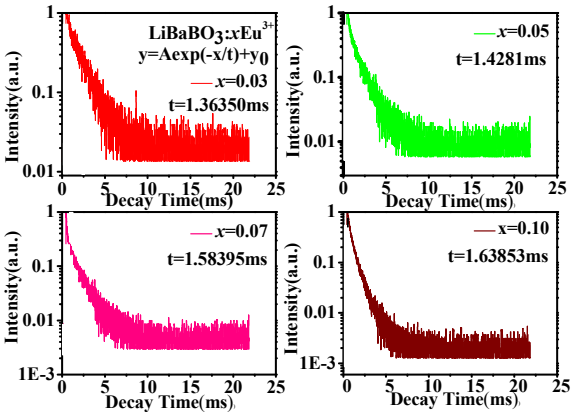

Figure 5 Decay curves of the $LiBaBO_3$:xEu^{3+} (x = 0.03, 0.05, 0.07, 0.10) phosphors (λ_{ex}= 396 nm, λ_{em}= 616 nm).

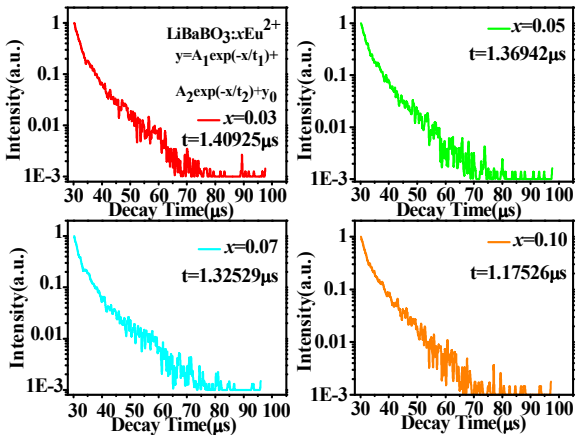

Figure 6 Decay curves of the $LiBaBO_3$:xEu^{2+} (x = 0.03, 0.05, 0.07, 0.10) phosphors (λ_{ex}= 350 nm, λ_{em}= 500 nm).

3.4. Luminescence properties of Tb doped materials

The Tb^{3+} ion exhibits efficient green luminescence in $LiBaBO_3$. Figure 7(a) shows the emission spectra at 240 nm excitation and (b) shows the excitation spectra under 550 nm emission wavelength of reduced $LiBaBO_3$:0.07Tb phosphor. The $LiBaBO_3$:0.07Tb phosphor revealed a series of excitation peaks between 200 and 400 nm with the band maxima at 240 nm due to the d–f transition of Tb^{3+} ions, and the other peaks with a high intensity located at 284, 355 and 379nm belong to the $^5D_3$–$^7F_4$, $^5D_3$ –$^7F_5$ and $^5D_3$–$^7F_6$. When excitated an electron from a $4f_n$ ground state to the 5d-configuration, the left behind n – 1 electrons in the 4f-shell can not only stay behind in the ground state but also in a $4f_{n-1}$ excited state [18], so we obtained two higher excitation peaks of Tb^{3+}at 240 nm and 284 nm, besides, Tb^{3+} is a lanthanide with more than half filled 4f-shell, and when excitated an electron to the 5d-shell, the spin $\mathbf{S_d}$ of the 5d-electron can be oriented parallel or anti-parallel to the 7/2 total spin $\mathbf{S_f}$ of the 4f-shell. Thus, it yields a lower energy high spin [HS] (s=8/2) and a higher energy low spin [LS] (s= 6/2) level [20]. The spectra mainly consist of two big peaks of emission lines, i.e. typical emission of Tb^{3+} ions as shown in (a). The emission bands with a high intensity located at 550 nm, 492 nm which belong to the $^5D_4$ –$^7F_5$ and $^5D_4$–$^7F_6$ transitions. Besides, the dominant green color of the phosphor owing to the magnetic dipole (ΔJ = ±1) transition is located at about 550 nm, which can be explained by the large values of the reduced matrix element at J = 5 and the Judd–Ofelt theory [21, 22].

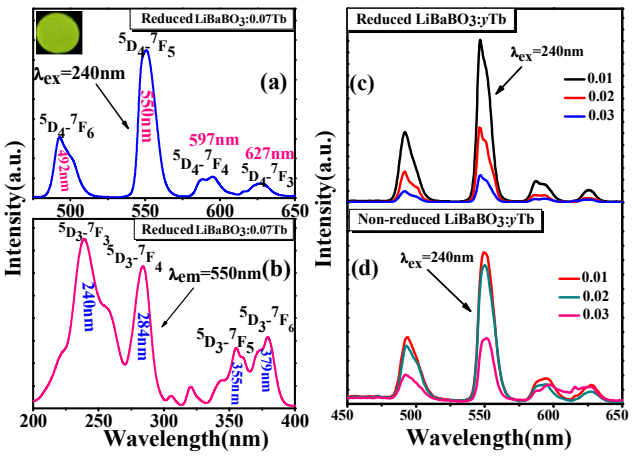

Figure 7 Emission (a) and excitation (b) spectra of $LiBaBO_3$:0.07Tb (λ_{ex}=240nm, λ_{em}=550nm); emission spectra of reducing (c) and non-reducing (d) $LiBaBO_3$:yTb (λ_{ex}=240nm).

To identify whether the reducing environment will have impact on Tb^{3+} ions in $LiBaBO_3$, $LiBaBO_3$:yTb (y=0.01, 0.02, 0.03) prepared in the air and in a thermal-reducing (H_2 + N_2) atmosphere, and the two emission spectrums of $LiBaBO_3$:yTb is shown in Figure 7 (c) and (d) (λ_{ex}=240nm). By comparing the spectral characteristics of the emission bands in the two spectrums, it is easily seen that the shapes and positions of the emission bands are almost the same. The main emission bands of Tb^{3+} ion in $LiBaBO_3$ were almost the

same. Thus, when doping Tb in the host of $LiBaBO_3$, the reduction or non-reduction had no influence on it. Besides, from the obtained emission spectra, it is evident that the intensity of $LiBaBO_3$:Tb^{3+} phosphors decreased with increasing Tb^{3+} ion concentration which is mainly caused by the non-radiative energy migration between two neighbouring Tb^{3+} ions through ion–ion interactions at high concentration. Hence, the intensity decreases with increasing Tb^{3+} concentration.

3.5. Luminescence properties of Eu^{3+} and Tb^{3+} doped materials and energy transfer between Eu^{3+} and Tb^{3+} ions

Figure 8 (a) (b) depicts the emission and excitation spectra of the as-prepared $LiBaBO_3$:0.03Eu^{3+}, *y*Tb^{3+}phosphor in the air. Monitored at 616 nm, the sample shows a lot of excitation bands from 200 to 475 nm and with a maximum at 396nm due to the $^7F_0$–$^5L_6$ transition of the Eu^{3+} ions. At the excitation of 396 nm, the excitation spectrum shows an intense red emission band attributed to the $^5D_0$–$^7F_2$ transition of the Eu^{3+} ion.

Generally, the Tb^{3+} ion is used as an activator in green phosphors, whose emission is mainly due to transitions of $^5D_3$→^7F_J in the blue region and $^5D_4$→^7F_J in the green region (J = 6, 5, 4, 3, 2) depending on its doping concentration [22]. In order to show the tunable luminescence, we can co-dope different rare earth ions by varying their concentrations [23]. In our experiment, we not only added *y*Tb^{3+} ions into $LiBaBO_3$:Eu^{3+} host, but also added *x*Eu^{3+} ions into $LiBaBO_3$:Tb^{3+} host. We found the emission and excitation spectra of the obtained phosphors were almost the same (the emission and excitation spectra of $LiBaBO_3$:0.03Tb, *x*Eu as shown in the supporting information Figure S2). Here, we chose $LiBaBO_3$:0.03Eu, *y*Tb prepared in the air to study.

As reported in many references [24-27], it is expected that an efficient energy transfer can occur from Tb^{3+} ions to Eu^{3+} ions. In order to investigate the effect of Tb^{3+} doping concentration on luminescence properties, a series of $LiBaBO_3$:0.03Eu^{3+}, *y*Tb^{3+} (*y*=0, 0.01, 0.02, 0.03, 0.05, 0.07, 0.10) phosphors were synthesized. Figure 8 illustrates the emission spectra measured at 396 nm and excitation spectra measured at 616 nm of the $LiBaBO_3$:0.03Eu^{3+}, *y*Tb^{3+}phosphor with different concentrations. It is obvious that high increases of the emission intensity when doped with Tb^{3+} ions, which is due to the fact that the luminescence intensities of various rare-earth ions can be enhanced or quenched by the energy transfer from other co-doped rare-earth ions [28-30]. And the red emission of the Eu^{3+} increases gradually and reaches a maximum at *x* = 0.05. With further increment of Tb^{3+} concentration, the emission intensity begins to decrease. On increasing the Tb^{3+} ion concentration, the distance between Tb^{3+} and Eu^{3+} ions decreased, thus the energy transfer between Tb^{3+} ions became less pronounced. According to the Dexter's energy transfer theory [31], the critical distance between the Eu^{3+} ions and Tb^{3+} ions can be calculated using the following equation [32]:

$$R=2[\frac{3V}{4\pi N y_c}]^{1/3} \quad (4)$$

where V is the volume of the unit cell, N represents the number of sites that the Eu^{3+} and Tb^{3+} occupy in per unit cell, and y_c is the critical concentration of Tb^{3+}. For $LiBaBO_3$ host, V = 298.2 Å^3, N = 4, and y_c = 0.05. Therefore, the critical distance R_C is calculated to be 14.176 Å. In oxide phosphor, non-radiative energy transfer usually occurs as a result of exchange interaction or multipole-multipole interaction [33]. Since the exchange interaction comes into effect only when the distance between activators is shorter than 5 Å, the mechanism of the emission intensity decreasing of Eu^{3+} ions and Tb^{3+} ions in the phosphor is dominated by multipole-multipole. Thus, we speculate the energy transfer occur from Tb^{3+} to Eu^{3+} ions under 396 nm excitation wavelength and 616 nm emission wavelength.

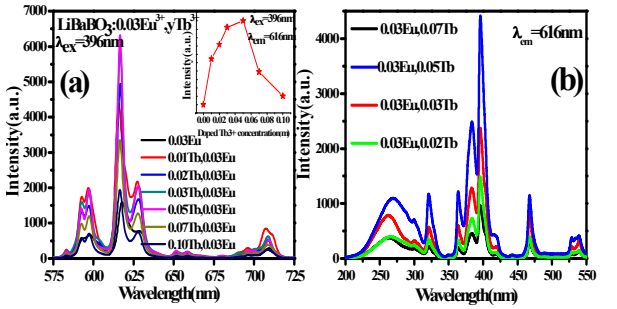

Figure 8 Emission spectra (a) and excitation spectra (b) of $LiBaBO_3$:0.03Eu^{3+}, *y*Tb^{3+} (*y* represents various doped concentration of Tb^{3+}). Inset (a) shows the emission intensity as a function of doped Tb^{3+} concentration (λ_{ex}=396 nm, λ_{em}=616 nm).

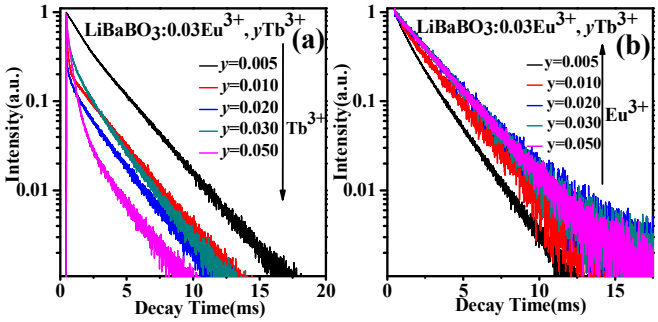

Figure 9 Decay curves of the $LiBaBO_3$:0.03Eu^{3+}, *y*Tb^{3+} (*y*=0.005, 0.010, 0.020, 0.030, 0.050) phosphors under λ_{em}=550 nm, λ_{ex}= 377 nm (a) and λ_{ex}=396 nm, λ_{em}=616 nm (b).

Table 1 Calculated lifetime of theTb^{3+} (t_1) and Eu^{3+} ion (t_2) of $LiBaBO_3$:0.03Eu^{3+}, yTb^{3+} phosphors

Samples	Lifetime(t_1)(ms)	Lifetime(t_2)(ms)
0.03Eu^{3+},0.005Tb^{3+}	3.9031	1.4551
0.03Eu^{3+},0.010Tb^{3+}	3.2887	1.7571
0.03 Eu^{3+},0.020 Tb^{3+}	3.1341	1.9462
0.03 Eu^{3+},0.030 Tb^{3+}	2.7563	1.9740
0.03 Eu^{3+},0.050 Tb^{3+}	1.8202	2.1088

In order to determine and estimate the energy transfer efficiency (ETE) from Tb^{3+} to Eu^{3+} , the decay profiles were carried out under 377 nm excitation wavelength and 616 nm emission wavelength, as shown in Figure 9. The decay curves were fitted to a single exponential function. By comparing and estimating, the average lifetimes of the single exponential curves was calculated by the formula (2) which is given previous. The calculated lifetimes of Eu^{3+} (t_2) and Tb^{3+} (t_1) are presented in Table 1. From the obtained lifetimes, it is evident that the lifetime of Tb^{3+} phosphors decreased while the lifetime of Eu^{3+} phosphors correspondingly increased with increasing Tb^{3+} ion concentration for the $LiBaBO_3$ samples co-doped with Eu^{3+} ions, suggesting that the energy transfer indeed occurred between Tb^{3+} and Eu^{3+} ions. It is noticeable that a considerable energy transfer occurred from Tb^{3+} to Eu^{3+} when the concentration of Tb^{3+} reaches 0.05. Those illustrate the occurrence of energy transfer from Tb^{3+} to Eu^{3+} when they are co-doped in the $LiBaBO_3$ host and provide a necessary condition for synthesizing the single phase tunable-color phosphors.

3.6. Luminescence properties of Eu^{2+} doped materials

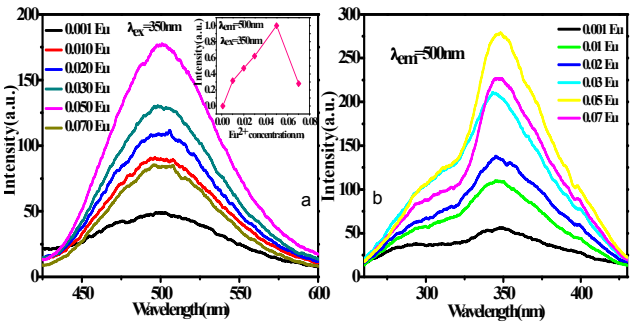

Figure 10 Emission spectra (a) and excitation spectra (b) for $LiBaBO_3$:xEu^{2+} (*x* represents various Eu^{2+} concentrations (*x*=0.001, 0.01, 0.02, 0.03, 0.05, 0.07). Inset: the emission intensity as a function of Eu^{2+} concentration.

Figure 10 presents the emission (a) and excitation spectra (b) for $LiBaBO_3$:xEu^{2+} (*x* represents various Eu^{2+} concentration) (*x*=0.001, 0.01, 0.02, 0.03, 0.05, 0.07). Inset (a) shows the emission intensity doped Eu^{2+} concentration at 500 nm. When measured at 350 nm, the emission spectrum shows an intense blue emission band attributed to the $^4f_6{}^5d_1 \rightarrow {}^4f_7$ transition of the Eu^{2+} ion. Figure 10 also shows the blue emission intensity of the Eu^{2+} increases gradually and reaches a maximum at *x* = 0.05. However, with further increment of Eu^{2+} concentration, the emission intensity begins to decrease. As we all know, non-radiative energy transfer usually occurs as a result of multipole-multipole interaction in oxide phosphors. According to Van Uitert's report, the emission intensity (I) per activator ion follows the equation [34]:

$$\frac{I}{x} = \frac{K}{[1+\beta(x)]^{\theta/3}} \quad (5)$$

where I represents the quenching intensity; x represents Eu^{2+} concentration; k and β represent constants for individual electric multipolar interactions; θ= 6, 8, and 10,and represents the dipole-dipole, dipole-quadrupole, and quadrupole-quadrupole interactions respectively. By the formula (5), log(I/x) acts a liner function of log(x) with a slop of (−θ/3). To get the value of θ, the relationship between log(I/x) and log(x) is plotted with x ranging from 0.005 to 0.05. From Figure 11, the value θ was determined to be 5.23416 from the slope (θ/3) which is close to 6.The result indicates that the concentration quenching mechanism of the Eu^{2+} emission in $LiBaBO_3$ host is dominated by the dipole−dipole interaction.

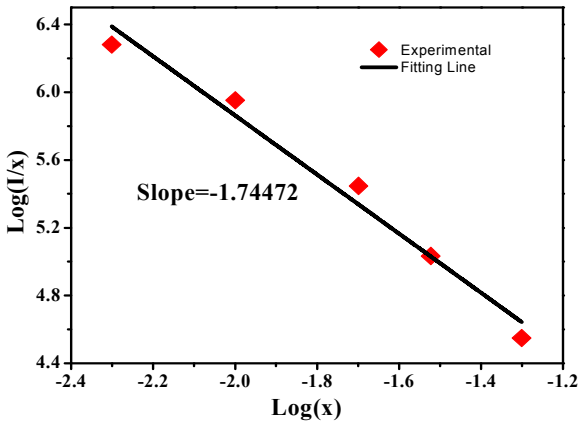

Figure 11 Dependence of log(I/x) on log(x) in $LiBaBO_3$:Eu^{2+} phosphors.

3.7. Luminescence properties of $LiBaBO_3$:Eu, Tb phosphor and energy transfer between the Eu^{2+}, Tb^{3+} and Eu^{3+} ions

Figure 12(a) illustrates the emission spectra of the inferior reductive $LiBaBO_3$:0.03Eu, *y*Tb phosphor. The emission spectrum measured at 350 nm exhibits a broad band and several narrow peaks. The broad band from400 to 575 nm centered at 500 nm is ascribed to the $^4f_6{}^5d_1 \rightarrow {}^4f_7$ transitions of the Eu^{2+} ions [35], while the peaks in the wavelength ranging from 580 to 650 nm are due to $^5D_0 - {}^7F_J$ (J = 0,1, 2, 3, and 4) from Eu^{3+}. However, Tb^{3+}-related emission spectrum is undetectable in the spectrum of $LiBaBO_3$:0.03Eu, *y*Tb because of the energy transfer. In order to prove Tb^{3+} indeed existing in the substance, the monitor at 550 nm which is the typical emission of the Tb^{3+} ions due to its $^5D_4 - {}^7F_5$ transition was taken, as shown in the Figure 12(b). When measured at 550 nm, the excitation spectrum of $LiBaBO_3$:0.03Eu, *y*Tb displays a strong broad band peaking at 377 nm. Besides, a comparison of excitation spectra was taken in order to prove that terbium ions indeed exist in the composition as shown in Figure 13. When monitoring at 550 nm in single-doped of Tb^{3+}, excitation spectrum is a broad range (330-400nm) with the peak at around 377nm, and the excitation has a broader band spectrum (300-450nm) with the same position peak in the co-doped of Tb and Eu measured at 550 nm, compared to excitation spectrum of co-doped of Tb and Eu measured at 500 nm, which is the characteristic

peak of Eu^{2+} [36]. The difference between the spectrums can be explained by the coexistence of $Eu^{2+}$and Tb^{3+}.

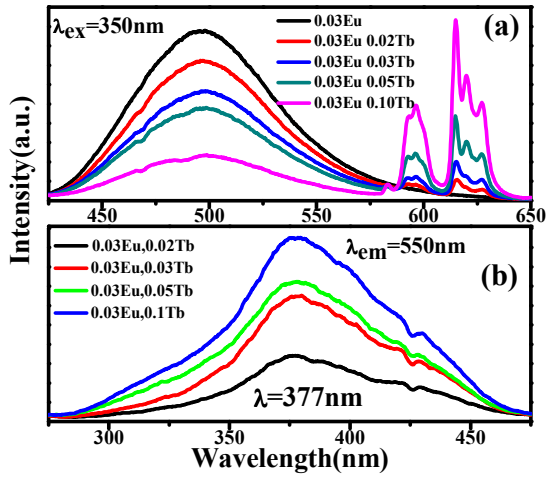

Figure 12. Emission(a) and excitation (b) spectra of $LiBaBO_3$:0.03Eu, yTb (y=0,0.02,0.03,0.05,0.10) .

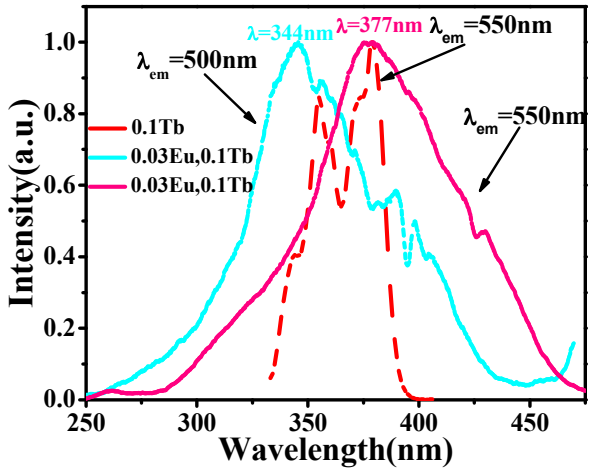

Figure 13 Comparison of excitation spectra of $LiBaBO_3$

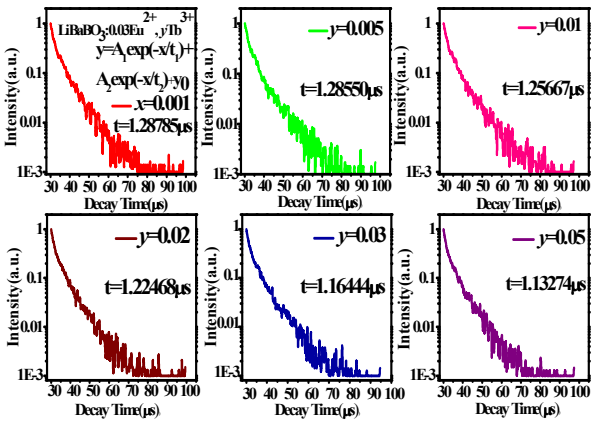

Figure 14 Decay curves of Eu^{2+} in $LiBaBO_3$:0.03Eu, yTb (y= 0.001, 0.005, 0.01, 0.02, 0.03, 0.05) phosphors (λ_{ex}=350 nm, λ_{em}=500 nm).

When the Tb content is increased in the $LiBaBO_3$:0.03Eu phosphor, the relative intensities of the green Eu^{2+} emission lines decrease gradually, and excitation peaks located at about 377nm appear to be accompanied by a increase of the green Tb^{3+}, indicating the efficient ET between Eu^{2+} and Tb^{3+}. However, Tb^{3+} ions do not show significant peak, because of the coexistence of Eu^{2+} and Eu^{3+}, and it had proved that Tb^{3+} can transfer energy to Eu^{3+}, so we can explain the changes in the emission spectrum in Figure 12 by energy transfer of $Eu^{2+} \rightarrow Tb^{3+} \rightarrow Eu^{3+}$.

From the analysis of emission and excitation spectra in the $LiBaBO_3$:0.03Eu, *y*Tb phosphor, it is clear that Eu^{2+}, Tb^{3+} and Eu^{3+} coexist in the single-phase $LiBaBO_3$ phosphors and that energy transfer can occur. To learn more about the dynamics of energy tranfer processes, luminescence decay curves of the Eu^{2+} (Figure14) and Eu^{3+} (Figure15) ions in $LiBaBO_3$:0.03Eu, *y*Tb phosphors were measured.

From Figure14, we can see that all the decay curves were fitted to the double exponential rule. The average fluorescence lifetimes of the Eu^{2+} ions in phosphors with different doping concentration of the Tb^{3+} are calculated by using equation (3). The calculated lifetimes are presented in Figure 14, and the life time becomes shorter with the increase of the Tb^{3+} ions because of the ET from Eu^{2+} to Tb^{3+}.

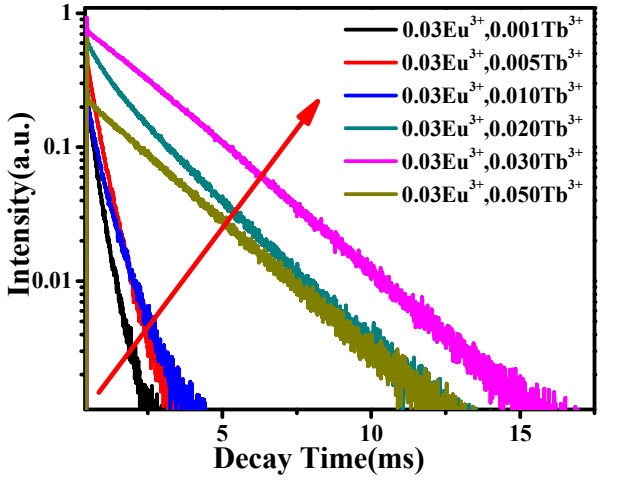

Figure 15 Decay curves of Eu^{3+} in $LiBaBO_3$:0.03Eu, *y*Tb (*y*= 0.001, 0.005, 0.010, 0.020, 0.030, 0.050) phosphors (λ_{ex}=396 nm, λ_{em}=616 nm).

By the same, all the decay curves were fitted to the single exponential rule of Eu^{3+}. The average fluorescence lifetimes of the Eu^{3+} ions in phosphors with different doping concentration of the Tb^{3+} are calculated by using the following equation [37]:

$$t=\frac{\int_0^\infty I(t)tdt}{\int_0^\infty I(t)dt} \quad (6)$$

where the I(t) represents the luminescence intensity at time t. So the lifetimes of the Eu^{3+} ions are1.36445, 1.51389, 1.61856,

Table 2 Calculated lifetime of the Eu^{2+} (t_1) and Eu^{3+} (t_2) ion and the energy transfer efficiency of the Eu^{2+} (η_1) and Eu^{3+} (η_2) ion of $LiBaBO_3$:0.03Eu , *y*Tb phosphors.

Samples	Lifetime (t_1) (μs)	η_1=1-t/t_0	Phosphor	Lifetime (t_2) (ms)	η_2=1-t/t_0
$0.03Eu^{2+}$	1.40925	0	$0.03Eu^{3+}$	1.36350	0
$0.03Eu^{2+}$, $0.001Tb^{3+}$	1.28785	0.0861	$0.03Eu^{3+}$, $0.001Tb^{3+}$	1.36445	0.0007
$0.03Eu^{2+}$, $0.005Tb^{3+}$	1.28550	0.0878	$0.03Eu^{3+}$, $0.005Tb^{3+}$	1.51389	0.0993
$0.03Eu^{2+}$, $0.010Tb^{3+}$	1.25667	0.1083	$0.03Eu^{3+}$, $0.01Tb^{3+}$	1.61856	0.1576
$0.03Eu^{2+}$, $0.020Tb^{3+}$	1.22468	0.1310	$0.03Eu^{3+}$, $0.02Tb^{3+}$	2.19399	0.3785
$0.03Eu^{2+}$, $0.030Tb^{3+}$	1.16444	0.1737	$0.03Eu^{3+}$, $0.03\ Tb^{3+}$	2.40227	0.4324
$0.03Eu^{2+}$, $0.050Tb^{3+}$	1.13274	0.1962	$0.03Eu^{3+}$, $0.05\ Tb^{3+}$	2.88193	0.5269

3.19399, 3.40227 and 3.88193ms for the $LiBaBO_3$:0.03Eu, *y*Tb phosphors with *y*=0.001, 0.005, 0.010, 0.020, 0.030 and 0.050, respectively. Energy transfer efficiency between the Eu^{2+} and Tb^{3+} ions (η_1) and between Tb^{3+} and Eu^{3+}ions (η_2) was also obtained from the decay lifetime by using the equation [38]:

$$\eta=1-t/t_0 \quad (7)$$

where t and t_0 are the lifetimes of sensitizer ion with and without the presence of activator, respectively. The lifetimes and energy transfer efficiencies are shown in Table 2. It is obvious that the energy transfer efficiencies between Eu^{2+} and Tb^{3+} (η_1) increased with the concentration of Tb^{3+} increased. As the same, the energy transfer efficiencies between Tb^{3+} and Eu^{3+} (η_2) also increased with the concentration of Tb^{3+} increased. And we also can see that η_1 is almost less than η_2, which can further explain why there is not emission spectrum of Tb^{3+}.

For a more intuitive explanation of the energy transfer between Eu^{2+}, Tb^{3+}, Eu^{3+}, we compare the lifetime values which calculated before, and we find that the lifetime values have a great different between the single-doped and co-doped of the host. For Eu^{3+}, $t_{Eu}{}^{3+}$=1.3635ms when we dope $0.03Eu^{3+}$ only in $LiBaBO_3$, compared $t_{Eu}{}^{3+}$=1.4551, 1.7571, 1.9462, 1.9740 ms for $LiBaBO_3$:$0.03Eu^{3+}$, *y*Tb^{3+}(*y*=0.01, 0.02, 0.03, 0.05), and when Eu^{2+}, Tb^{3+}, Eu^{3+} coexist in $LiBaBO_3$, the lifetime values become 1.61856, 2.19399, 2.40227, 2.88193 ms. However, for Eu^{2+}, $t_{Eu}{}^{2+}$=1.40925 μs when we dope $0.03Eu^{2+}$ only in $LiBaBO_3$, and the value decreases when Eu^{2+}, Tb^{3+}, Eu^{3+} coexist in the host which are 1.25667, 1.22468, 1.16444, 1.132745 μs. By contrast, we further demonstrate the energy transfer actually took place between Eu^{2+}, Tb^{3+} and Eu^{3+}.

3.8. Mechanism of energy transfer from Eu^{2+} to Eu^{3+} in Eu^{2+} → Tb^{3+} → Eu^{3+}

We first suppose the cascade model of terbium chain (Tb^{3+}–Tb^{3+}–Tb^{3+}–...) to explain the mechanism of energy transfer from Eu^{2+} →Tb^{3+} →Eu^{3+}. In this case, if the energy transfer probability between Tb atoms is p (0<p < 1), then the probability (P) of terbium chain energy transfer will be p^n, for the reason that the probability for the cascade energy transfer goes down exponentially from ref [39]. However, from Figure 7 (a) and (b), the overlap between the emission and excitation spectra of Tb^{3+} is very low, resulting in the probability (p) of energy transfer between Tb^{3+} to Tb^{3+} is very low [40–42]. But in this study, the energy transfer from Eu^{2+} →Tb^{3+} →Eu^{3+} is relatively considerable, so we bring forward the branch model to explain the process of energy transfer for the terbium bridge [43], as shown in Figure 16. First, when Eu^{2+} ions excited by UV light, it will give out a blue emission and sensitize Tb^{3+} ions in the ground state. Then, the excited Tb^{3+} ions may give out a green emission and transfer energy to Eu^{3+}, at the same time, the excited Tb^{3+} ion may release energy in the way of cross-relaxation with another Tb^{3+} ion in the ground state, and the Tb^{3+} which absorbed the energy from excited Tb^{3+}will also flow to Eu^{3+} through the process of energy transfer.

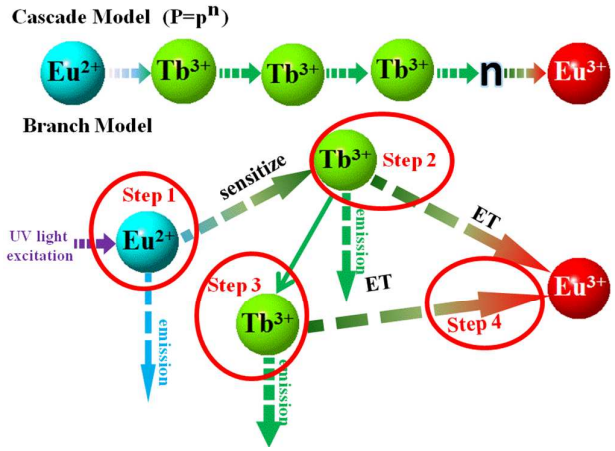

Figure 16 Energy transfer models of terbium chain (cascade model) and terbium bridge(branch model).

The Eu^{3+} ions are sensitized by Tb^{3+} unaffected by the procedure that is followed, which is consistent with the decreasing average time of Tb^{3+} in Figure 9 and Table 1. Moreover, the excitation spectra of $LiBaBO_3$:$0.03Eu^{3+}$, *y*Tb^{3+}in Figures 8(a) demonstrate that the main emission of Eu^{3+} originates from the $^5D_3$ (377–398 nm) and energy levels of Tb^{3+}, corresponding to step2 and step 4 in Figure 16.

The energy transfer of Tb^{3+}→Eu^{3+} is efficient, however, the efficiency of energy transfer in Eu^{2+}→Tb^{3+} is relatively poor. Therefore, it is necessary to raise the content of Tb^{3+} to shorten the average distance of Tb^{3+}-Eu^{3+} and increase the probability of energy transfer in step2 and step 4. Furthermore, the decay time of Eu^{2+} is as short as microseconds, while the values for Tb^{3+} and Eu^{3+} are on

the order of milliseconds, so Tb^{3+} ions also can play the role of storing the energy for Eu^{3+} [44, 45].

3.9. Color-tuning luminescence properties of $Eu^{2+}/Tb^{3+}/Eu^{3+}$ activated $LiBaBO_3$

According to the data of emission spectra of the samples and the colorimetric standard promulgated by International Lighting Commission in 1931, we calculated CIE color coordinates of the sample of $LiBaBO_3$:0.10Eu^{3+}, $LiBaBO_3$:0.10Tb^{3+} and $LiBaBO_3$:0.10Eu^{2+} were (0.6475, 0.3591), (0.2515, 0.6409) and (0.1575, 0.2276), respectively, indicating that the samples have good red, green, or blue emission performance when single-doping Eu^{3+}, Tb^{3+} or Eu^{2+}. We can obtain different colors when co-doping the ions [46], such as we can get the colors from green to red when co-doping Tb^{3+} and Eu^{3+}, or from blue to red when co-doping Eu^{2+} to Eu^{3+}, similarly, we can obtain the colors from green to blue when co-doping Tb^{3+} and Eu^{2+}. Thus, we make sure that $LiBaBO_3$ is a potential host to apply LEDs with doping the right ions concentration.

4. Conclusions

In summary, a series of $Eu^{2+}/Tb^{3+}/Eu^{3+}$activated $LiBaBO_3$ phosphors have been synthesized and investigated. The $LiBaBO_3$ host has a monoclinic cell with cell parameters of a = 6.372 Å, b = 7.022 Å, c = 7.058 Å, β = 113.89 °, and Z= 4. Under near-UV excitation, the host shows different but intensive luminescence when doped Eu^{3+}, Tb^{3+}, Eu^{2+} respectively. For $LiBaBO_3$, the energy transfer can occur between Tb^{3+} to Eu^{3+} in the host prepared in the air. Besides, Eu^{2+} and Eu^{3+} can coexist in an inferior reductive atmosphere and the color changes along with the vary concentrations. Importantly, when co-doped with Tb and Eu in the same condition, energy transfer of $Eu^{2+} \rightarrow Tb^{3+} \rightarrow Eu^{3+}$ occurred and we obtained different colors of light. The obtained phosphors have excellent luminescence properties, and high color purity features. Based on these reasons, the phosphors may be promising candidates for applications in LEDs lighting.

5. Acknowledgements

The work is supported by the National Natural Science Foundation o f China (No.50902042), the Funds for Distinguished Young Scientists of Hebei Province, China (No.A2015201129), the Natural Science Fo undation of Hebei Province, China (Nos.A2014201035, E201420103 7), the Education Office Research Foundation of Hebei Province, Chi na (Nos.ZD2014036, QN2014085), the Midwest Universities Compre hensive Strength Promotion Project.

6. Notes and references

[1] M. Shang, C. Li, and J. Lin, *Chem. Soc. Rev.*, 2014, 43(5), 1372-1386.
[2] Y. Q. Li, A. C. A. Delsing, G. de With, H. T. Hintzen, *Chem. Mater.*, 2005, 17 (12), 3242–3248.
[3] Y. Zhang, D. Geng, X. Kang, M. Shang, Y. Wu, X. Li, H. Lian, Z. Cheng, J. Lin, *Inorg. Chem.* 2013, 52, 12986−12994.
[4] X. Liu, C. Li, Z. Quan, Z. Cheng, J. J. Lin, *Phys. Chem. C* 2007, 111, 16601−16607.
[5] Y. Wang, M. G. Brik, P. Dorenbos, Y. Huang, Y. Tao, H. Liang, *J. Phys. Chem. C* 2014, 118, 7002−7009.
[6] C. Hecht, F. Stadler, P. J. Schmidt, J. r. S. auf der Günne, V. Baumann, W. Schnick, *Chem. Mater.* 2009, 21, 1595−1601.
[7] D. Hou, C. Liu, X. Ding, X. Kuang, H. Liang, S. Sun, Y. Huang, Y. Tao, *J. Mater. Chem. C.* 2013, 1, 493−499.
[8] S. Lizzo, A. Meijerink, G. J.Dirksen, G. Blasse, *J. Phys. Chem.* 1995, 56, 959.
[9] W. Lü, Z. Hao, X. Zhang, Y. Luo, X. Wang, J. Zhang, *Inorg. Chem.* 2011, 50, 7846−7851
[10] N. Guo, Y. Song, H. You, G. Jia, M. Yang, K. Liu, Y. Zheng, Y. Huang, H. Zhang, *Eur. J. Inorg. Chem.* 2010, 29, 4636−4642.
[11] D. Jia, R. Meltzer, W. Yen, W. Jia, X. Wang, *Appl. Phys. Lett.*2002, 80, 1535−1537.
[12] H. You, X. Wu, G. Hong, J. Tang, H. Hu, *Chem. Mater.* 2003, 15, 2000−2004.
[13] B. H. Lee, H. G. Jeong, K.-S. Sohn, *J. Electrochem. Soc.* 2010, 157, J227−J232.
[14] G. Santomauro, J. Baier, W.J. Huang, S. Pezold, J. Bill, *Acta Cryst. ,* 1976, A32, 751-767.
[15]Y. T. Li, X. H. Liu, *Materials Research Bulletin.,* 2015, 64, 88-92
[16]T. Grzyb, A. Gruszeczka, R. J. Wiglusz, Z. Sniadecki, B. Idzikowski S. Lis,*J. Mater. Chem.*, 2012, 22, 22989-22997
[17] B. Anthony, Parmentier, P. Dirk, *Materials. ,* 2013, 6, 3663-3675
[18] P. Dorenbos, *ECS J. Solid State Sci. Technol.*, 2013, 2, R3001–R3011.
[19] C.-H. Huang, T. M. Chen, *Opt. Express,* 2010, 18, 5089–5099.
[20] P. Dorenbos, *J. Alloys Compd.*, 2002, 341, 156–159.
[21] G. S. Ofelt, *J. Chem. Phys.*, 1962, 37, 511–520.
[22] B. R. Judd, *Phys. Rev.*, 1962, 127, 750–761.
[23] M. B. Xie, Y. Tao, Y. Huang, H. B. Liang and Q. Su, *Inorg. Chem.,* 2010, 49, 11317–11324.
[24] Z. L. Fu, X. J. Wang, Y. M. Yang, Z. J. Wu, D. F. Duan, and X.H. Fu, *Dalton Trans.*, 2014, 43, 2819-2827.
[25] Y. Tian, B. j. Chen, B. N. Tian, N. S. Yu, J. S. Sun, X. P. Li, J. S. Zhang, L. H. Cheng, H. Y. Zhong, Q. Y. Meng, R. N. Hua, *J. Colloid Interface Sci.,* 2013, 393, 44–52.
[26] K. Liu, H. P. You, Y. H. Zheng, G. Jia, Y. J. Huang, M. Yang, Y. H. Song, L. H. Zhang , H. J. Zhang, *Cryst. Growth Des.,* 2010, 10, 16–19.
[27] H. Guo, F. Li, R. F. Wei, H. Zhang , C. G. Ma, *J. Am. Ceram. Soc.,* 2012, 95, 1178–1181
[28] J. H. Huang, X. C. Wang, Y. D. Hou, X. F. Chen, L. Wu, X. Z. Fu, *Environ. Sci. Technol.,* 2008, 42, 7387–7391.
[29] J. E. Shelby, *J. Am. Ceram. Soc.,* 1983, 66, 414–416.
[30] Y. Wu, C. S. Shi, *J. Alloys Compd.,* 1995, 224, 177–180.
[31] D. Dexter, J. H. Schulman, *J. Chem. Phys.* 1954, 22, 1063−1070.
[32] G. Blasse, *Philips Res. Rep.* 1969, 24, 131_144.
[33] D. L. Dexter, *J. Chem. Phys.* 1953, 21, 836−850.

[34] N. Guo, H. You, Y. Song, M. Yang, K. Liu, Y. Zheng, Y. Huang, H. Zhang, *J. Mater. Chem.* 2010, 20, 9061–9067.
[35] J. R. Qiu, K. Miura, H. Inouye, S. Fujiwara, T. Mitsuyu, K. Hirao, *J. Non-Cryst.* 1999, 244, 185–188.
[36] G. Blasse, *J.Solid State Chem.* 1986, 62, 207–211.
[37] D. Wen, J. Shi, *Dalton Trans.* 2013, 42, 16621–16629.
[38] Y. Jia, W. Lu, N. Guo, W. Lu, Q. Zhao, H. You, *Chem. Commun.* 2013, 49, 2664–2666.
[39] Z. Xia, J. Zhuang, A. Meijerink, X. Jing, *Dalton Trans.* 2013, 42, 6327–6336.
[40] L. Zhang, J. Zhang, X. Zhang, Z. Hao, H. Zhao, Y. Luo, *ACS Appl. Mater.* 2013, 5, 12839–12846.
[41] C. Duan, Z. Zhang, S. Rösler, A. Delsing, J. Zhao, H. T. Hintzen, *Chem. Mater.* 2011, 23, 1851–1861.
[42] W. Lü, N. Guo, Y. Jia, Q. Zhao, W. Lv, M. Jiao, B. Shao, H. You, *Inorg. Chem.* 2013, 52, 3007–3012.
[43] M. Jiao, N. Guo, W. Lü, Y. Jia, W. Lv, Q. Zhao, B. Shao, H. You, *Inorg. Chem.* 2013, 52, 10340–10346.
[44] M. Shang, G. Li, X. Kang, D. Yang, D. Geng, J. Lin, *ACS Appl. Mater.* 2011, 3, 2738–2746.
[45] L. Zhang, J. Zhang, X. Zhang, Z. Hao, H. Zhao, Y. Luo, *ACS Appl. Mater.* 2013, 5, 12839–12846.
[46] A. Li, D. Xu, H. Lin, S. Yang, Y. Shao, Y. Zhang, Z. Chen, *RSC Adv.*, 2015, 5, 45693-45702.